

Accepted for publication in Polymer Degradation and Stability

Published in August 26, 2013

DOI: 10.1016/j.polymdegradstab.2013.08.011

**Thermooxidative Degradation of LDPE nanocomposites: Effect of Surface Treatments
of Fumed Silica and Boehmite Alumina**

E. Vuorinen^{1*}, N. Nhlapo¹, T. Mafa² and J. Karger-Kocsis^{2,3,4}

¹National Metrology Institute of South Africa, Private Bag X34, Lynnwood Ridge, 0040,
Republic of South Africa.

²Polymer Technology, Faculty of Engineering and the Built Environment,
Tshwane University of Technology, Pretoria 0001, Republic of South Africa

³MTA–BME Research Group for Composite Science and Technology, Muegyetem rkp. 3., H-
1111 Budapest, Hungary

⁴Department of Polymer Engineering, Faculty of Mechanical Engineering,
Budapest University of Technology and Economics, H-1111 Budapest, Hungary

Submitted to Polymer Degradation and Stability, March 2013

* Corresponding author: E. Vuorinen (E-mail: evuorin@nmisa.org)

Abstract

Fumed silica (FS) and synthetic boehmite alumina (BA) with and without surface treatments were incorporated in 5 wt. % in low density polyethylene (LDPE) through melt blending. FS was treated by hexadecyl silane, whereas BA by octyl silane and alkylbenzene sulfonic acid. The related nanocomposites were subjected to pyrolysis gas chromatography-mass spectrometry (Py-GC-MS) and thermogravimetric analysis (TGA) under isothermal and dynamic conditions, respectively. Py-GC-MS results proved that the thermal degradation mechanism did not change in presence of the nanofillers. The latter suppressed the formation of high molecular weight hydrocarbons and affected the relative amounts of diene/alkene/alkane fragments for each hydrocarbon fraction.

Dynamic TGA scans were registered at different heating rates in air. The activation energy (E_a) of thermoxidative degradation was calculated by the Ozawa-Flynn-Wall (OFW) method at various degradation degrees. E_a of the LDPE nanocomposites depended on both specific surface area and surface treatment of the nanofillers used. The former enhanced whereas the latter decreased the activation energy for the LDPE-FS nanocomposites. By contrast, E_a was slightly increased for the surface treated LDPE-BA nanocomposites.

Keywords: low-density polyethylene (LDPE), thermal degradation, nanocomposites, silica, boehmite, surface treatment

1. Introduction

Modification of polymers by various nanoparticles has attracted vivid interest in both academia and industry. This is due to the property improvements achieved at remarkably low nanofillers content. Property improvements may cover both structural (mostly mechanical performance) and functional properties (e.g. various conductivities). The fillers are of organic and inorganic natures and their size, at least in one direction, is in the nanometer range. Like

traditional fillers, the nanoparticles can be categorized upon their aspect ratio. Accordingly, one can differentiate between spherical, platy and fibrous fillers. The outstanding property profile of nanocomposites is attributed to the size, dispersion characteristics of the nanoparticles and to the onset of favorable filler/matrix interactions [1].

Incorporation of nanofillers usually increased the resistance to thermal, thermooxidative degradations of the corresponding nanocomposites. This was usually reflected by a shift toward higher temperatures in the related thermogravimetric analysis (TGA) traces when comparing those of the plain and nanomodified polymer, respectively. This behavior was reported for low density and linear low density polyethylene (LDPE and LLDPE, respectively) modified with copper nanoparticles [2], layered double hydroxides [3-4], layered silicates (clays) [3,5-6], silica [5], chalk [7], multiwall carbon nanotubes [8-9], alumina [10-11] and boehmite alumina [12-13]. Similar results were reported for fumed silica filled high density PE nanocomposites [14-15]. By contrast, graphene caused an adverse effect that was traced to the presence of physisorbed water [16]. Note that the above listed nanoparticles cover spherical, platy and fibrous ones, as well. The observed enhancement in the thermooxidative stability was attributed to the hampered diffusion of oxygen and volatile decomposition products in- and outward, respectively, in the nanocomposites.

Accordingly, the delayed thermal degradation should depend on the shape (aspect ratio) and specific surface area of the nanoparticles. The latter govern the filler/matrix interactions. In fact, platy (disk-type) fillers, such as layered silicates [5] and fibrous (needle-like) ones, such as carbon nanotubes [8-9], markedly enhanced the resistance to thermooxidation, and even to fire. Comparing the thermal stability of LDPE/copper nano- and microcomposites it was found that the nanoparticles are more efficient “thermooxidative additives” than the microscaled ones [2]. The surface treatment of the particles should influence the thermooxidative stability of the matrix, as well. This occurs by two ways: i) changing the dispersion, and ii) improving the matrix/filler interactions. In order to separate the above effects and thus get a deeper insight in the effects of surface treatments nanocomposites with such nanoparticles should be selected which can well be dispersed also without surface treatments.

It was reported that fumed silica (FS) can be finely dispersed in polyethylene and surface treatment does not alter its dispersion characteristics [15,17]. Synthetic boehmite alumina (BA) has a similar feature. BA can also be homogeneously and finely dispersed in PEs without surface treatment [12, 18]. It has to be underlined, however, that the mean size of

the dispersed nanoparticles (being agglomerates) is a multitude of the primary one and its value increased with the filler loading. Nonetheless, both FS and BA can be finely and homogeneously dispersed in polyethylenes as demonstrated before [12,15,17-18]. There is a large difference in the specific surface area of the above nanofillers: FS has a doubled value of BA. Further, there is a difference in their aspect ratios, too. FS exhibits an aspect ratio of 1, whereas that of BA, though disk-shaped, is a markedly larger one. However, the related agglomerates are of spheroid appearance in both cases and thus comparable. Therefore these nanofillers, viz. FS and BA, with and without surface treatments were selected to study their effects on the thermooxidative stability of LDPE. FS was treated with hexadecyl silane, whereas BA with octyl silane and alkylbenzene sulfonic acid, respectively. Thermooxidative stability of LDPE nanocomposites, containing 5 wt.% filler, was studied by pyrolysis gas chromatography-mass spectrometry (Py-GC-MS) and thermogravimetric analysis (TGA). The decomposition was studied in both isothermal (Py-GC-MS) and dynamic (TGA) conditions. TGA traces were registered at different heating rates in order to calculate the apparent activation energy of the thermal decomposition.

2. Experimental

2.1 Materials and sample preparation

LDPE grade LT388 (melt flow index at 190°C/2.16 kg: 10 dg/min; density: 0.922 g/cm³) from Sasol (Sasolburg, South Africa) was used as matrix in this study. As unmodified fumed hydrophilic silica, Aerosil® 200 (FS), whereas as surface treated, Aerosil® R816 (FS-C16) – both from Evonik Industries, Hanau, Germany – were used. FS-C-16 was modified by hexadecyl silane to make it hydrophobic. FS characteristics, listed in Table 1, show that their mean primary particle size is identical and there is only a marginal change in their BET surface area. The synthetic boehmite alumina (BA) was Disperal® 40 (primary crystallite size was ~40 nm) from Sasol GmbH (Hamburg, Germany). BA with the chemical composition AlO(OH) was used in pristine and in surface modified forms. BA surface treatment occurred by octyl silane (BA-C8) and by C10–C13 alkylbenzene sulfonic acid (BA-C10-13BS), respectively. Characteristics of BA are also listed in Table 1.

The above nanofillers were incorporated in 5 wt.% in LDPE. Nanocomposites were prepared via melt compounding using a Haake Rheomix OS internal mixer (Thermo Fischer Scientific, Karlsruhe, Germany). Mixing lasted for 8 min at 175°C at 60 revolutions per minute (rpm).

Table 1

Characteristics of the nanofillers used according to their producers' data

Designation	Product	BET surface area [m ² /g]	Primary particle size [nm]
FS	Aerosil® A200	200±25	12
FS-C16	Aerosil® R816	190±20	12
BA	Disperal® 40	101	43
BA-C8	Disperal® 40 experimental	~100	~40
BA-C10-13BS	Disperal® 40 experimental	~100	~40

2.2 Measurements

2.2.1 Py-GC-MS

Pyrolysis-GC-MS analysis was performed by a Thermo Trace GC Ultra coupled to a Thermo Trace DSQ from Thermo Scientific and CDS 100 Pyroprobe. The column was first held at 40 °C for 1 min then heated at 20 °C/min to 250 °C and held there for 10 min. The interface temperature was 300 °C and pyrolysis temperature 700 °C. Restek Rxi-5ms/15 m/0.25 mmID column was used in this study. Helium was used as a carrier and as a pyrolysis gas.

2.2.2 TGA- FTIR

A Cahn Versa Thermo HM TGA device interfaced with a Nicolet Nexus 470 Fourier transform infrared (FTIR) bench was used. A custom-made connector prevented condensation of decomposition products (temperature about 100 °C). The 1.1 m evolved gas analysis (EGA) transfer line was unheated. A small pump was used to draw the gas from TGA to the gas cell. Nitrogen was used as a purge gas. The samples weighed typically 50 ± 5 mg and the temperature was raised from room temperature to 700 °C in a 50 ml flow in air at heating rates of 5, 10 and 20 °C/min. The gas cell was placed in the IR scanning path for the detection of decomposition products. The gas cell was controlled by ThermoNicolet

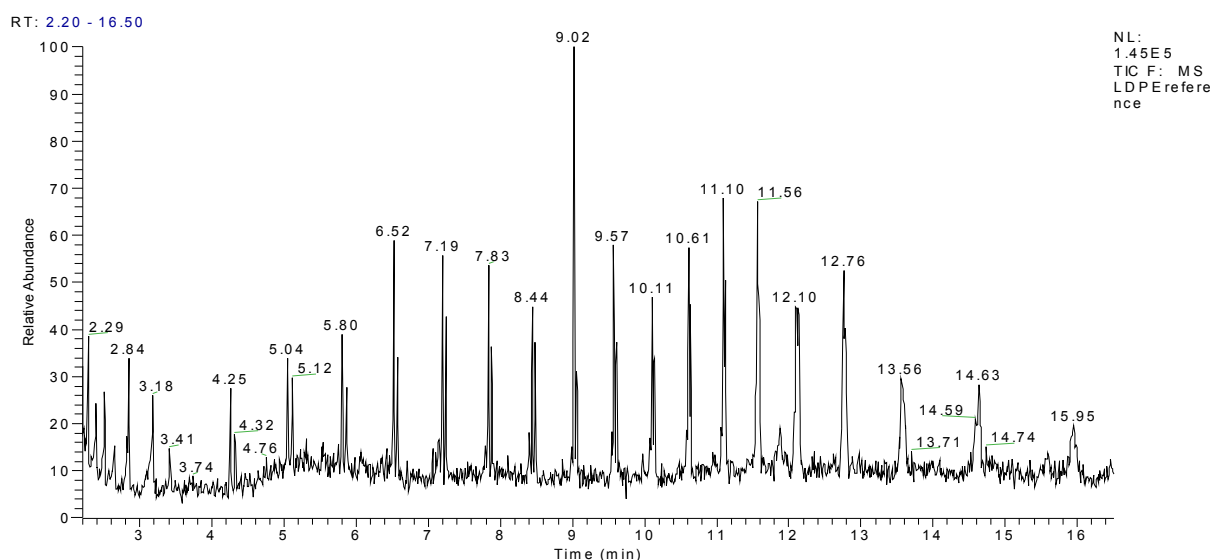
FTIR/TGA interface and kept at room temperature. IR detection was between 600 and 4000 cm^{-1} . The spectra were taken as an average 50 scans at 8 wavenumber resolution. Sampling interval was 27 seconds.

3. Results and discussion

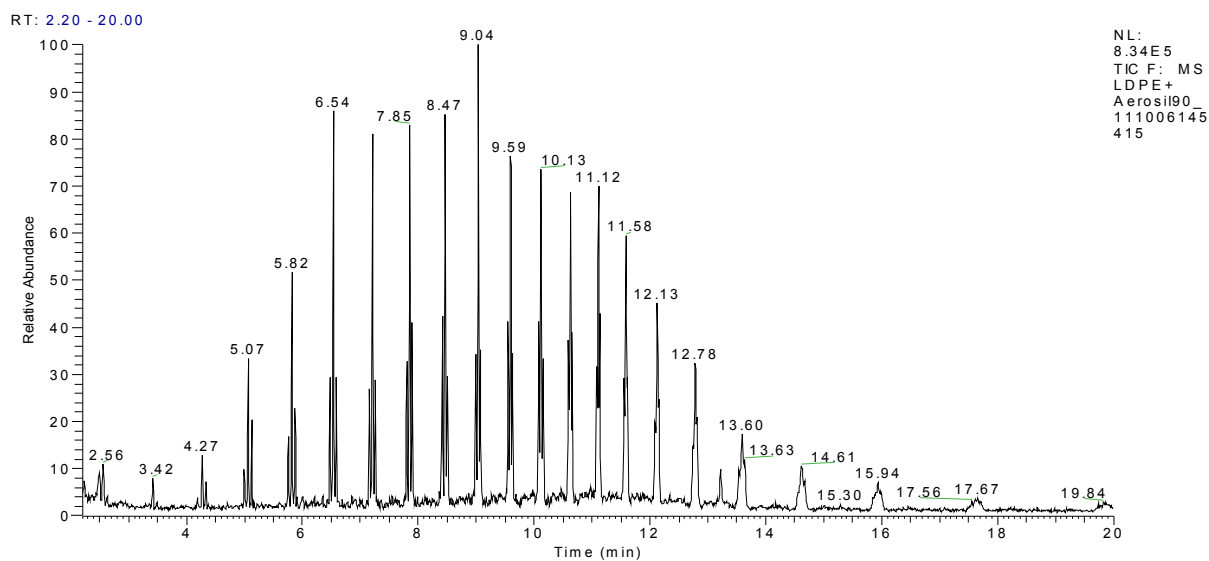
3.1 Py-GC-MS

3.1.1. LDPE/fumed silica nanocomposites

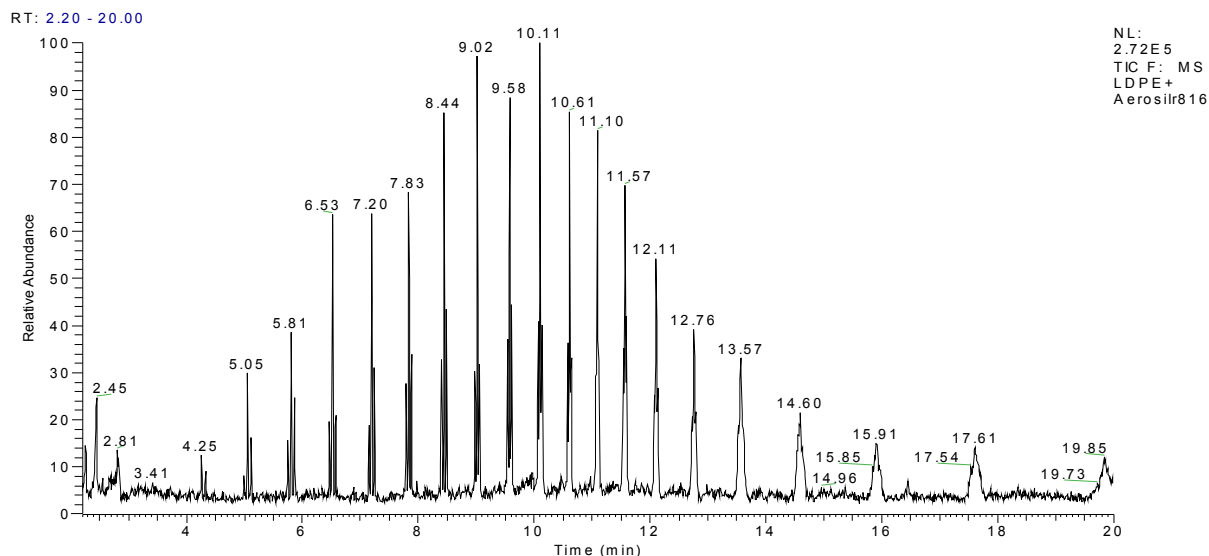
Pyrograms registered during the thermal degradation of LDPE and its FS and FS-C16 nanocomposites are compared in Figure 1(a-c).



(a). LDPE Reference



(b). LDPE/FS nanocomposite

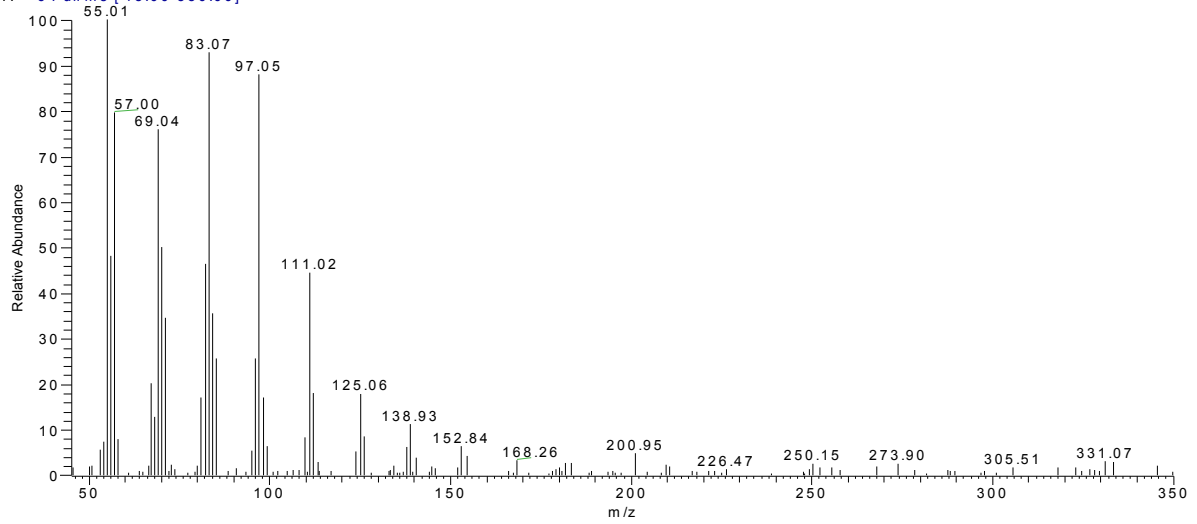


(c). LDPE/FS-C16 nanocomposite

Figure 1: Pyrograms of the degradation products of the LDPE and its fumed silica nanocomposites. Designations: (a) LDPE reference, (b) LDPE/FS nanocomposite and (c) LDPE/FS-C16 nanocomposite

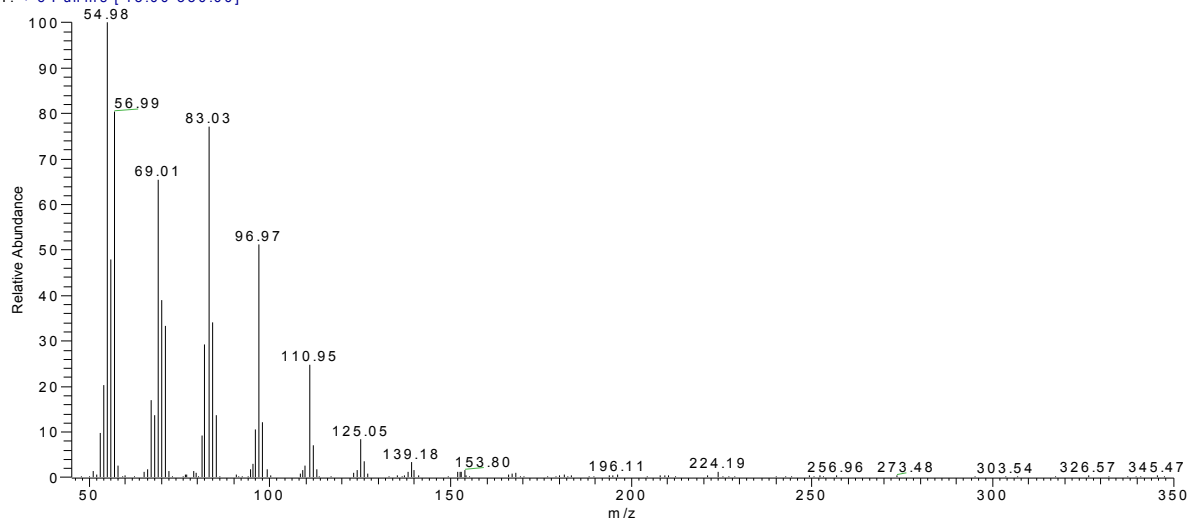
One recognizes already at the first glance that there is no prominent change in retention time peaks. The only difference is linked with the relative amount of the evolved gases. This suggests that the presence of fumed silica, with and without surface treatment, did not affect the thermal decomposition pathway. It is widely accepted [19-21] that the thermal degradation of polyethylene starts with random scission fragmenting the original polymer backbone. The length of these molecular fragments composed mostly of alkenes and alkanes, vary in a broad range. Recall that dienes and alkenes are formed by beta-scission of the primary macroradicals, whereas their intermolecular hydrogen transfer yields alkanes. The degradation pathway is well documented in the literature [20-21]. Higher resolution of the pyrograms in Figure 1 would resolve that the retention time peaks cover triplets. This becomes obvious when showing the corresponding mass spectra – cf. Figure 2.

LDPE reference #668 RT: 9.02 AV: 1 NL: 1.38E4
T: + c Full ms [45.00-350.00]

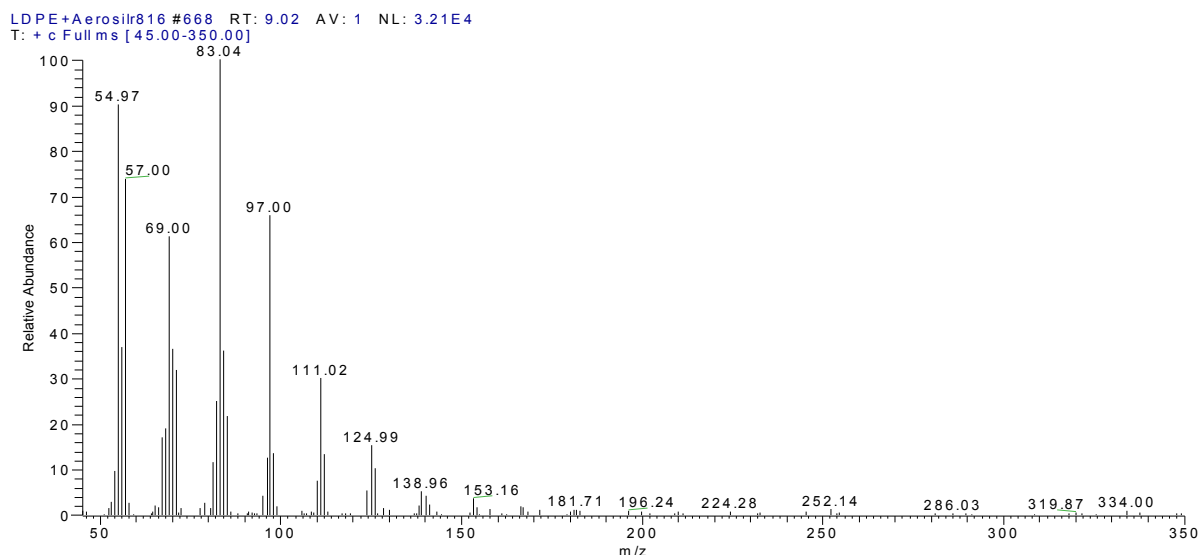


(a). LDPE Reference

LDPE+Aerosil90_111006145415 #670 RT: 9.04 AV: 1 NL: 1.10E5
T: + c Full ms [45.00-350.00]



(b). LDPE/FS



(c). LDPE/FS-C16

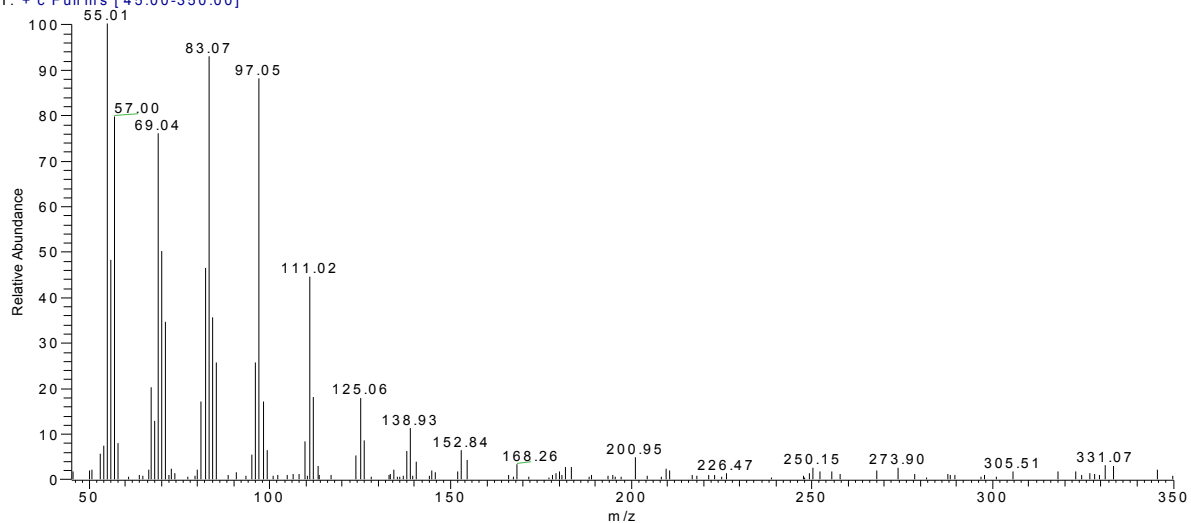
Figure 2: Characteristic mass spectra of the decomposition products of (a) LDPE, (b) LDPE/FS and (c) LDPE/FS-C16.

In the triplets the first peak is assigned to diene, the second to alkene, while the third to alkane at a given hydrocarbon fraction [20-21]. The first triplet in Figure 2 is linked with the C4 fraction. Note that the m/z values of butadiene, butene and butane are 54, 56 and 58, respectively. The other peaks can be easily assigned to the corresponding hydrocarbon fractions since the peaks follow at intervals of 14 mass units, representing a methylene group. The MS traces in Figure 2 highlight that the formation of high molecular weight hydrocarbons, i.e. higher than C13 fractions, are markedly reduced in presence of FS.

3.1.2. LDPE/boehmite alumina nanocomposites

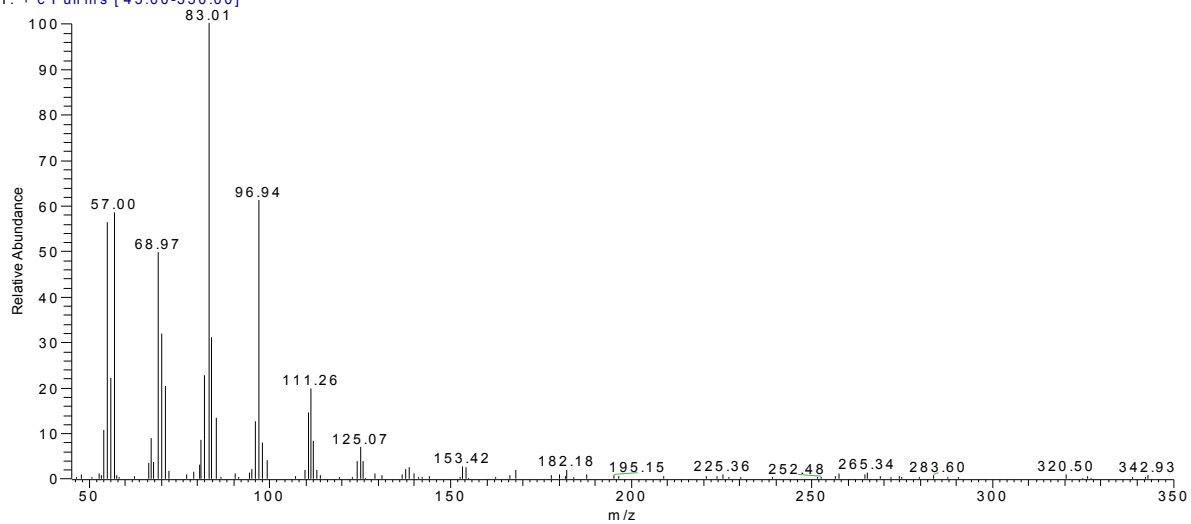
Similar mass spectra were obtained for the BA-filled nanocomposites. By contrast to the LDPE/FS series both C-8 and C10-13BS treatments of BA resulted in slightly enhanced high molecular weight hydrocarbon fractions compared to the untreated BA – cf. Figure 3.

LDPE reference #668 RT: 9.02 AV: 1 NL: 1.38E4
T: + c Fullms [45.00-350.00]

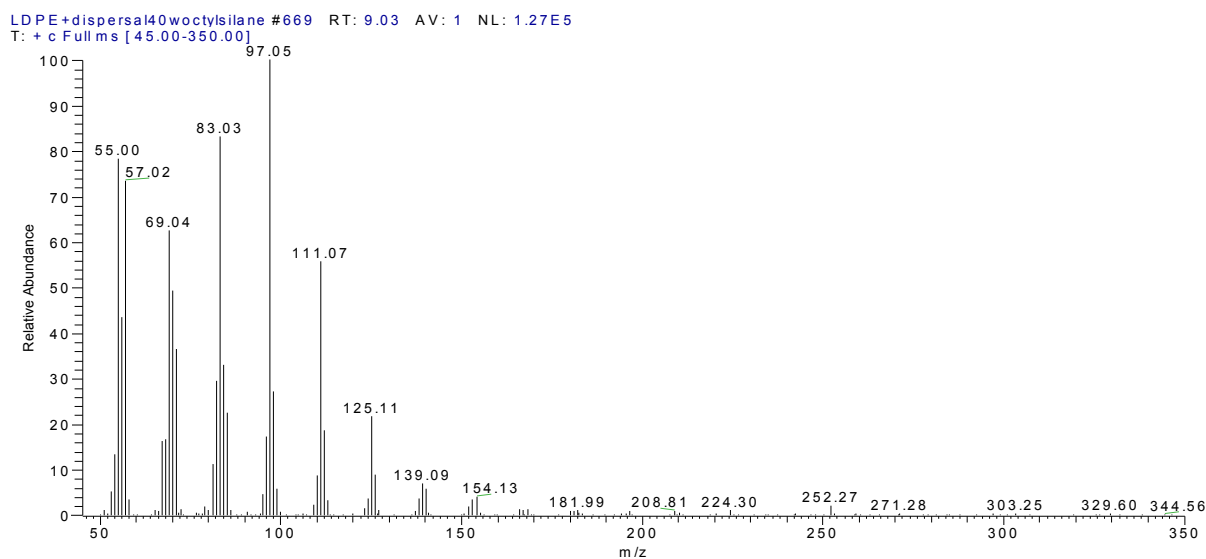


(a). LDPE Reference

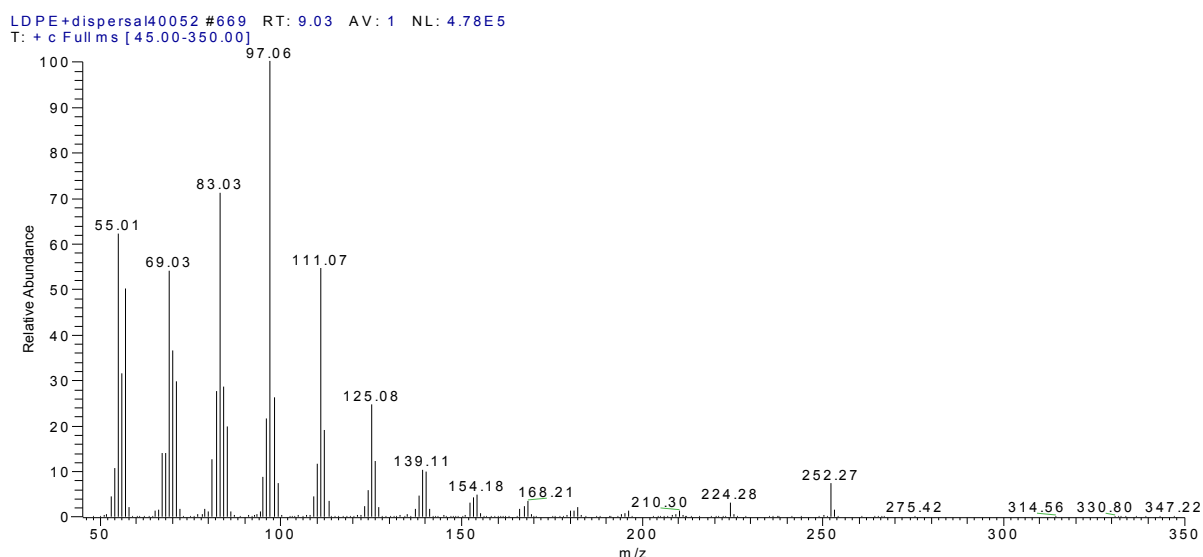
LDPE+Dispera40 #669 RT: 9.03 AV: 1 NL: 2.27E4
T: + c Fullms [45.00-350.00]



(b). LDPE/BA



(c). LDPE/BA-C8



(d). LDPE/BA-C10-13BS

Figure 3: Characteristic mass spectra of the decomposition products of (a) LDPE, (b) LDPE/BA, (c) LDPE/BA-C8 and (d) LDPE/BA-C10-13BS.

3.2 TGA-FTIR

The TGA combined with IR is a type of Evolved Gas Analysis (EGA) system. When a sample is heated in the TGA, the sample will release volatile materials, which are transferred to the IR cell, where the components are identified.

TGA onset temperature indicates the temperature at which the weight loss begins. It was found in this study that the addition of FS nanoparticles enhances the thermal stability of

LDPE (Table 2). For the LDPE/BA nanocomposite a similar tendency was found except the data measured at 20 °C/min

Table 2

TGA onset temperatures for the LDPE and its nanocomposites

Sample	Onset Temperatures (°C)		
	Heating rate (5°C/min)	Heating rate (10°C/min)	Heating rate (20°C/min)
LDPE	377	400	476
LDPE/ FS	408	446	485
LDPE/FS-C16	402	457	476
LDPE/BA	376	461	466
LDPE/BA-C8	400	443	470
LDPE/BA-C10-13BS	413	443	467

The degradation profile of LDPE and its nanocomposites was followed from the analysis of the evolved volatile products. The Gram-Schmidt (GR) plots (e.g. Figure 4) show the total change in the infrared signal relative to the initial state. They provide information related to the total infrared absorbance of the evolved components over the entire spectral range.

3.2.1. LDPE/fumed silica nanocomposites

Figure 4 shows the TGA traces, i.e. residual mass (in %) and derivative mass loss (in mg/min) as a function of temperature (in °C). This figure also displays those data which were derived to characterize the thermal decompositions of the samples. These parameter are: temperatures belonging to 2, 25, 50 and 75 % mass losses ($T_{d,2}$, $T_{d,25}$, $T_{d,50}$ and $T_{d,75}$, respectively), peak temperatures of the derivative mass loss and Gram-Schmidt intensity (denoted by T_p and $T_{p,G-s}$, respectively). Figure 4 highlights that LDPE degrades in one single step practically without any residue.

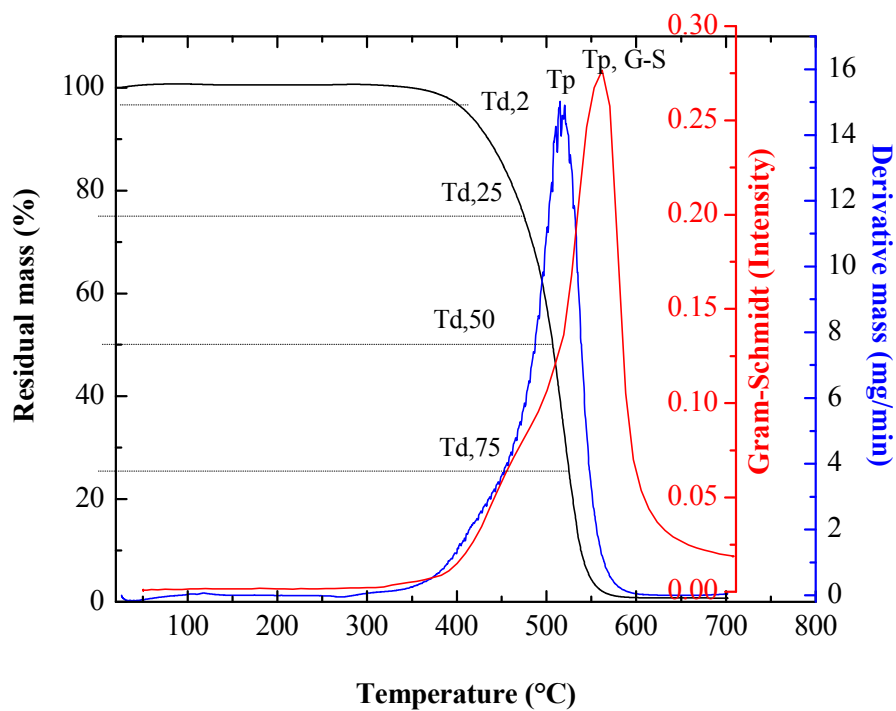


Figure 4: TGA traces and Gram-Schmidt (G-S) diagram on example of the plain LDPE.

Note: this figure indicates the data read from the TGA measurements

Incorporation of FS did not influence the TGA response except causing some temperature delay – cf. Figure 5. Like LDPE, the thermal decomposition of the LDPE/FS nanocomposites occurred in one step. Comparing the TGA traces in Figure 5 one can recognize, that the related TGA curves along with the GR plots were shifted toward higher temperatures. On the other hand, the effect of the surface treatment of FS was marginal on these traces.

Data determined from the TGA measurements are summarized in Table 3.

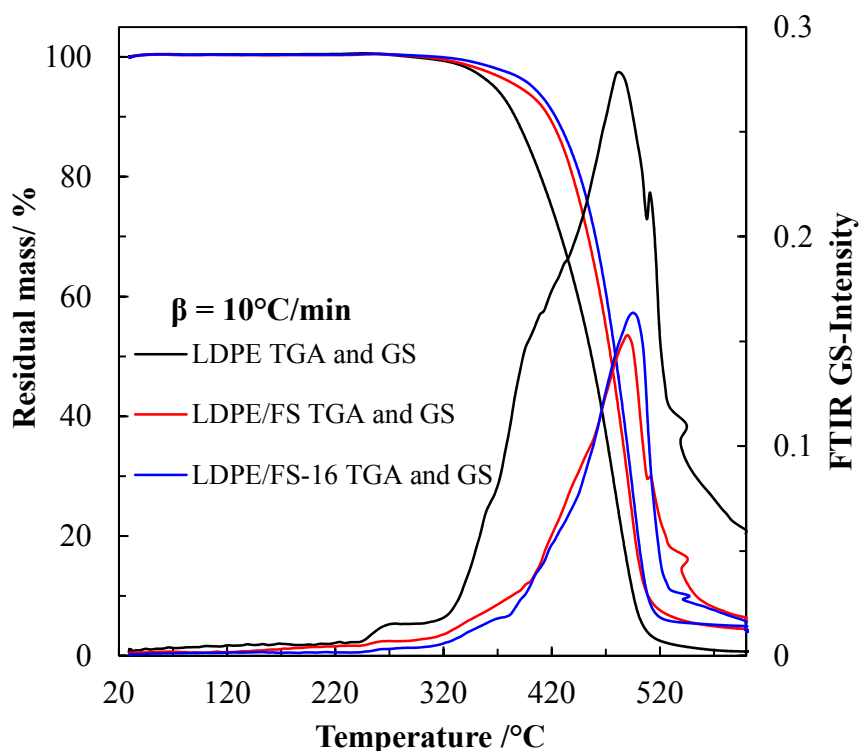


Figure 5: TGA traces and Gram-Schmidt (G-S) diagrams of the LDPE, LDPE/FS and LDPE/FS-C16 nanocomposites registered at 10 °C/min heating rates. Note: the residue agrees fairly with the nanofillers amount introduced

Table 3

TGA data determined for the LDPE and its nanocomposites containing FS and BA nanoparticles with and without surface treatments

Material	Heating rate, β [°C/min]	TGA data						
		$T_{d,2}$ [°C]	$T_{d,25}$ [°C]	$T_{d,50}$ [°C]	$T_{d,75}$ [°C]	Residue [%]	T_p [°C]	$T_{p,G-S}$
LDPE	5	337.3	398.8	427.2	451.6	0.271	444	487.5
	10	344	419.8	456.6	480.9	0.648	579.1	479.9
	20	389.6	474.7	506.6	525.0	0.456	515.2	550.6
LDPE/FS	5	326.1	424.3	450.1	472.6	3.207	468.7	478
	10	353.5	447.1	474.3	493.2	4.132	488.8	490.1
	20	395.3	489.4	516.7	534.5	0.463	528.7	540.9

LDPE/FS- C16	5	319.5	414.8	444	465.1	2.809	463.6	465.5
	10	369.9	454	478.9	496.5	4.121	493.1	495.3
	20	406.2	494.8	520.5	538.9	4.386	531.6	550.5
LDPE/BA	5	331.5	401.9	432.6	459.6	3.911	441.1	452.2
	10	392.1	459.1	491.4	512.9	4.989	503.4	511.9
	20	368.1	470.7	505.1	526.1	3.658	517.7	530.2
LDPE/BA- C8	5	327.4	408.4	437.9	461.7	4.6017	459	467.1
	10	357.4	439.9	471.6	492.5	4.4892	490.2	498.1
	20	388.8	478.9	510.3	530.5	4.4496	520.4	551.8
LDPE/BA- C10-13BS	5	373.5	424.5	444.9	460.9	3.4648	452.7	458.8
	10	380.7	448.4	475.7	494.4	3.4345	493.8	502.7
	20	417.4	743.6	505.4	524.6	3.114	519.7	534.5

3.2.2. LDPE/boehmite alumina nanocomposites

Effects of the BA nanofillers were similar to FS as demonstrated on the TGA behaviors of the related nanocomposites in Figure 6. The corresponding results are listed again in Table 3. Recall that the observed stabilization, i.e. the shift in the TGA traces toward higher temperature, is generally attributed to the shielding effect of the nanoparticles in the evolution of the gases during thermal decomposition [14].

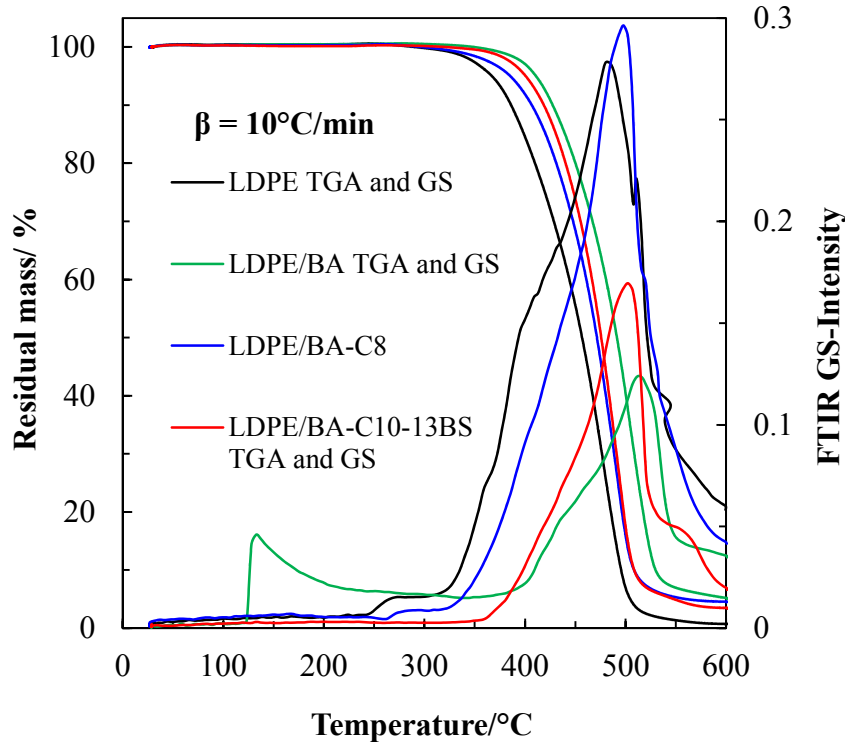


Figure 6: TGA traces and Gram-Schmidt (G-S) diagrams of the LDPE, LDPE/BA, LDPE/BA-C8 and LDPE/BA-C10-13BS nanocomposites registered at 10 °C/min heating rates. Note: the residue agrees fairly with the nanofillers amount introduced

3.2.3. Activation energy of the thermooxidative degradation of the nanocomposites

By using the dynamic TGA data, measured at different heating rates, the activation energy can be calculated by using the method credited to Ozawa, Flynn and Wall (OFW) [14, 22]. This approach, belonging to the integral isocoverisional methods, assumes that the reaction rate at a given extent of conversion (α , in our case degradation) is only function of temperature. Accordingly, the temperature dependence of the isoconversional rate can be used to determine the related activation energy (E_α). Note that this does not imply the consideration of any reaction model and thus called “model-free” method [22]. Adapting the OFW method requires to measure the temperatures corresponding to fixed α values ($T_{\alpha,i}$) from experiments performed at different heating rates (β_i). Based on the OFW approach, given by:

$$\ln \beta_i = \text{Const.} - (E_\alpha/RT_{\alpha,i}) \quad \text{Equation (1)}$$

Plotting $\ln \beta_i$ against $1/T_{\alpha,i}$ should give a straight line and its slope is directly proportional to the activation energy ($-E_\alpha/R$), where $T_{\alpha,i}$ is the absolute temperature linked to the fixed a

conversion and R denotes universal gas constant. Note that in many reports there is a multiplication constant, namely 1.052, before the second term in Equation 1 [14, 22].

To check whether or not E_a is independent of the conversion, i.e. degradation degree, the following actual residual mass values were considered: 75, 50 and 25 %. They correspond to $T_{d,25}$, $T_{d,50}$ and $T_{d,75}$ “thermooxidative conversion” values, respectively. Recall that the related data are listed at different heating rates for all our systems in Table 3. Figure 7 shows on example of LDPE/BA-C10-13BS where these data were taken from.

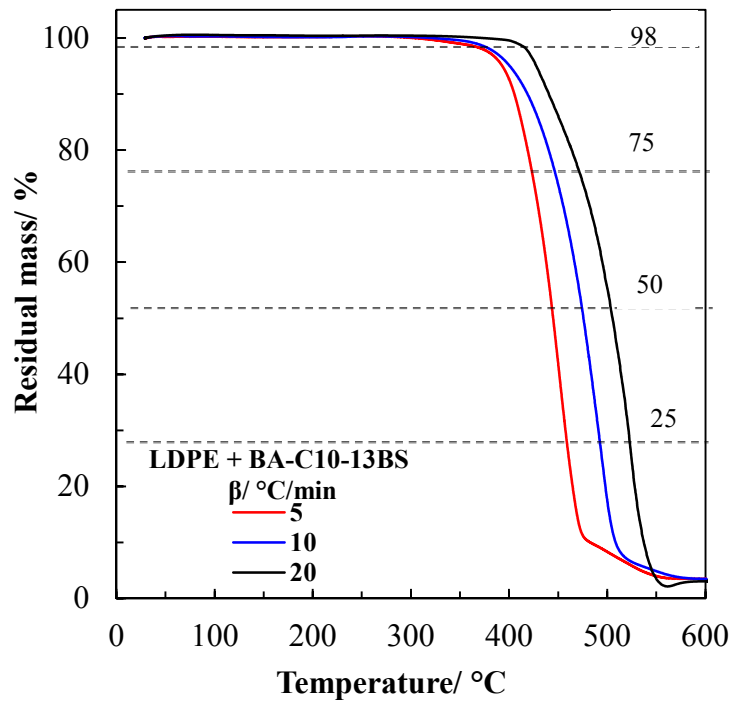


Figure 7: TGA traces of the registered at $\beta=5, 10$ and 20 °C/min, respectively, for the LDPE/BA-C10-13BS nanocomposite

The OFW treatise of the data taken from Figure 7 (see also Table 2) is given in Figure 8. One can observe that the $\ln \beta_i$ vs $1/T_{\alpha,i}$ data obey very well the linear regression presumed by the OFW method. Parameters of the linear regressions, along with the calculated activation energy (E_a) values are listed in Table 4.

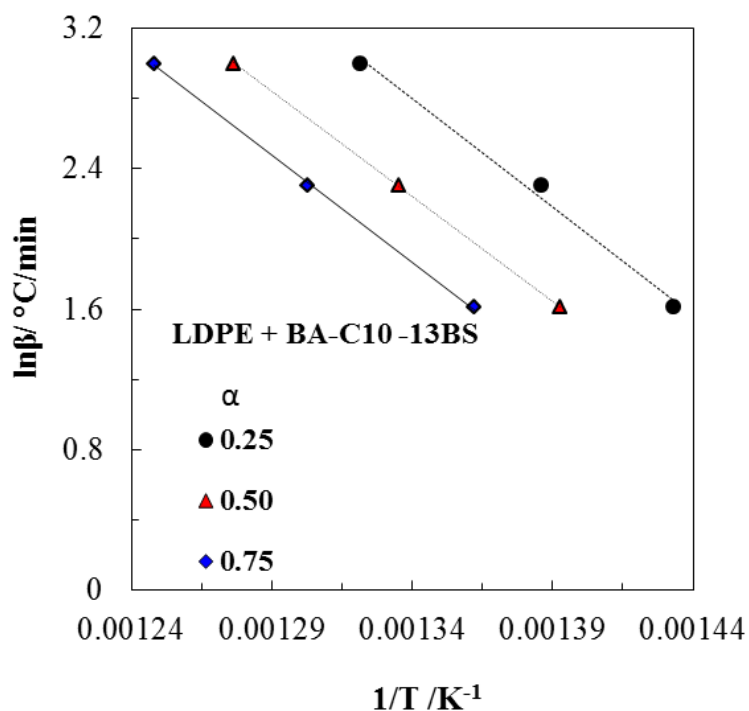


Figure 8: $\ln \beta_i$ vs $1/T_{\alpha,i}$ plotted for the LDPE/BA-C10-13BS nanocomposite at residual mass values 75, 50 and 25 wt.%. Note that the latter data correspond to $\alpha=0.25$, $\alpha=0.50$ and $\alpha=0.75$, respectively

Table 4

Values obtained from the OFW plots for the LDPE and LDPE nanocomposites studied

Material	Conversion, α [%]	Linear regression $y = a-bx$			E_a [kJ/mol]
		a	b	R^2	
LDPE	0.25	15.19	9092.26	0.9953	75.6
	0.50	15.23	9528.59	0.9997	79.2
	0.75	14.82	9337.00	0.9751	77.6
LDPE/FS	0.25	17.57	11078.9	0.9891	92.1
	0.50	17.90	11735.3	0.9914	97.6
	0.75	19.26	13099.9	0.9855	108.9

LDPE/FS-C16	0.25	14.90	9151.2	0.9998	76.1
	0.50	15.99	10309.4	0.9998	85.7
	0.75	16.84	11222.2	0.9983	93.3
LDPE/BA	0.25	14.51	8735.1	0.9292	72.6
	0.50	14.60	9201.9	0.9360	76.5
	0.75	15.55	10208	0.9367	84.9
LDPE/BA-C8	0.25	16.40	10067.7	0.9994	83.7
	0.50	16.61	10665.1	0.9999	88.7
	0.75	17.80	11885.2	0.9994	98.8
LDPE/BA-C10-13BS	0.25	19.66	12565.3	0.9970	104.5
	0.50	18.22	11923.8	0.9999	99.1
	0.75	17.51	11673.5	0.9999	97.1

The results in Table 4 show that the activation energy values slightly increase with increasing conversion. This is in accordance with the general trend found for the thermal degradation of polymers and related nanocomposites. However, E_a does not increase monotonously for LDPE and the activation energy of LDPE/BA-C10-13BS follows an adverse tendency. If we would consider the scatter in the E_a data within their 95% confidence limits the applicability of the OFW approach could be, however, substantiated.

In the present study the activation energy values are markedly lower (at about their halves) than those published in the literature for LDPE [23]. The obvious reason for that is that our LDPE was highly branched facilitating easy chain scissions. Entanglement of the long alkyl chains of the silane modifier in FS-C16 with molecules of LDPE matrix yielded lower E_a values for LDPE/FS-C16 than those found for LDPE/FS. One can thus conclude that pure physisorption of the matrix molecules on the FS nanoparticles' surface prominently enhance the resistance to thermal degradation. Surface treatment supporting intensive chain intermingling with the matrix molecules does not affect the apparent activation energy compared to the matrix.

The scenario is somewhat different for the BA nanocomposites. First, the untreated BA practically does not influence the activation energy of the thermal decomposition of LDPE. This is in harmony with the low specific surface of BA. Recall that the specific surface area of

BA was at about the half of FS. The effect of BA is restricted for some time/temperature delay in the degradation – cf. data in Table 3. Further, it is intuitive that octyl chains in BA-C8 are less prone for creating entanglements with the LDPE molecules than C16 chains on FS. The change in the E_a values of LDPE/BA-C10-13BS as a function of the conversion can be attributed to the initially high resistance of the C10-13BS chains.

4. Conclusion

This work was devoted to study the thermal degradation behavior of low density polyethylene (LDPE) based nanocomposites with fumed silica (FS) and boehmite alumina (BA) nanoparticles with and without surface treatments. FS was treated by hexadecyl silane (C16), whereas BA by octyl silane (C8) and alkylbenzene sulfonic acid (C10-13-BS). The nanocomposites were subjected to pyrolysis gas chromatography-mass spectrometry (Py-GC-MS) and thermogravimetric analysis (TGA) investigations. Based on the results achieved the following conclusions can be drawn:

- nanoparticles did not change the basic degradation pathway but affect the relative fractions of the volatile hydrocarbons. Thus, the improved thermooxidative stability, manifesting in a shift of the TGA curves toward higher temperatures, is of physical origin and due to the barrier effect of the nanoparticles hampering the diffusion of the gaseous degradation products
- FS caused a more prominent improvement in the thermal stability that was attributed to its higher specific surface compared to BA
- the apparent activation energy of the decomposition, assessed by the Ozawa-Flynn-Wall (OFW) method, was reduced when the surface coating agent (C16) was capable for chain entanglements with the PE. The surface treatment of BA had a marginal effect on the activation energy, even in different stages of the decomposition.

Acknowledgments

This work was supported by the scientific programs: "Development of quality-oriented and harmonized R+D+I strategy and functional model at BME" [TÁMOP 4.2.1/B-09/1/KMR-2010-0002]; and „Talent care and cultivation in the scientific workshops of BME" [TÁMOP 4.2.2/B-10/1-2010-0009].

References

- [1] Karger-Kocsis J in “Nano- and Micromechanics of Polymer Blends and Composites” (Eds: Karger-Kocsis J and Fakirov S), Hanser, Munich, 2010, Ch. 12, pp. 425-470.
- [2] Xia X, Cai S, Xie C. Preparation, structure and thermal stability of Cu/LDPE nanocomposites. *Mater Chem Phys* 2006; 95:122-129.
- [3] Qiu L, Chen W, Qu B. Morphology and thermal stabilization mechanism of LLDPE/MMT and LLDPE/LDH nanocomposites. *Polymer* 2006; 47:922-930.
- [4] Costa FR, Wagenknecht U, Heinrich G. LDPE/Mg-Al layered double hydroxide nanocomposites: Thermal and flammability properties. *Polym Degrad Stab* 2007; 92:1813-1823.
- [5] García N, Hoyos M, Guzmán J, Tiemblo P. Comparing the effect of nanofillers as thermal stabilizers in low density polyethylene. *Polym Degrad Stab* 2009; 94:39-48.
- [6] Zanetti M, Bracco P, Costa L. Thermal degradation behavior of PE/clay nanocomposites. *Polym Degrad Stab* 2004; 85:657-665.
- [7] Cao X, Gao J, Dai X, Liu Y, He X. Kinetics of thermal degradation of nanometer calcium carbonate/linear low-density polyethylene nanocomposites. *J Appl Polym Sci* 2012; 126:1159-1164.
- [8] Bocchini S, Frache A, Camino G, Claes M. Polyethylene thermal oxidative stabilization in carbon nanotubes based nanocomposites. *Eur Polym J* 2007; 43:3222-3235.
- [9] Barus S, Zanetti M, Bracco P, Musso S, Chiodoni A, Tagliaferro A. Influence of MWCNT morphology on dispersion and thermal properties of polyethylene nanocomposites. *Polym Degrad Stab* 2010; 95:756-762.
- [10] Ngu JLS, Noshida I, Akmil M, Luqman Chuah A, Chantar Theyv R. Thermal properties of low-density polyethylene/alpha-alumina nanocomposites. *J Thermoplast Compos Mater* 2011; 25:415-426.
- [11] Malucelli G, Palmero P, Ronchetti S, Delmastro A, Montanaro L. Effect of various nanofillers on the thermal and mechanical behaviour of low-density polyethylene -Al₂O₃ composites. *Polym Int* 2010; 59:1084-1089.
- [12] Khumalo VM, Karger-Kocsis J, Thomann R. Polyethylene/synthetic boehmite alumina nanocomposites: Structure, thermal and rheological properties. *Express Polym Lett* 2010; 4:264-274.

- [13] Pedrazzoli D, Ceccato R, Karger-Kocsis J, Pegoretti A. Viscoelastic behavior and fracture toughness of linear-low-density polyethylene reinforced with synthetic boehmite alumina nanoparticles. *Express Polym Lett* 2013 (submitted)
- [14] Chrissafis K, Paraskevopoulos KM, Pavlidou E, Bikiaris D. Thermal degradation mechanism of HDPE nanocomposites containing fumed silica nanoparticles. *Thermochim Acta* 2009; 485:65-71.
- [15] Dorigato A, Pegoretti A, Frache A. Thermal stability of high density polyethylene-fumed silica nanocomposites. *J Therm Anal Calorim* 2012; 109:863-873
- [16] Kim S, Do I, Drzal LT. Thermal stability and dynamic mechanical behavior of exfoliated graphite nanoplatelets-LLDPE nanocomposites. *Polym Compos* 2010; 31:755-761
- [17] Dorigato A, Pegoretti A. (Re)processing effects on linear low-density polyethylene/silica nanocomposites. *J Polym Res* 2013; 20:92.
- [18] Khumalo VM, Karger-Kocsis J, Thomann R. Polyethylene/synthetic boehmite alumina nanocomposites: structure, mechanical, and perforation impact properties. *J Mater Sci* 2011; 46:422-428.
- [19] Pielichowski K, Njuguna J. *Thermal Degradation Polymeric Materials*, Rapra, Shawbury, 2005, Ch.5, pp. 41-47
- [20] Bockhorn H, Hornung A, Hornung U, Schawaller D. Kinetic study on the thermal degradation of polypropylene and polyethylene. *J Anal Appl Pyrolysis* 1999; 48:93-109.
- [21] Serrano DP, Aguado J, Escola JM, Rodríguez JM, San Miguel G. An investigation into the catalytic cracking of LDPE using Py-GC/MS. *J Anal Appl Pyrolysis* 2005; 74:370-378.
- [22] Vyazovkin S, Burnham AK, Criado JM, Pérez-Maqueda LA, Popescu C, Sbirazzuoli N. ICTAC Kinetics Committee recommendations for performing kinetic computations on thermal analysis data, *Thermochim Acta* 2011; 520:1– 19.
- [23] Westerhout RWJ, Waanders J, Kuipers JAM, van Swaaij WPM. Kinetics of the low-temperature pyrolysis of polyethylene, polypropylene, and polystyrene, Modeling experimental determination, and comparison with literature models and data. *Ind Eng Chem Res* 1997; 36: 1955-1964